

## Biomedical Paper

# Ultrasound Registration of the Bone Surface for Surgical Navigation

Devin V. Amin, M.D., Ph.D., Takeo Kanade, Ph.D., Anthony M. DiGioia III, M.D., and  
Branislav Jaramaz, Ph.D.

*Center for Medical Robotics and Computer Assisted Surgery, The Robotics Institute, Carnegie Mellon University (D.V.A., T.K.), and Institute for Computer Assisted Orthopedic Surgery, Western Pennsylvania Hospital (A.M.D., B.J.), Pittsburgh, Pennsylvania*

### ABSTRACT

**Objective:** To allow non-invasive registration of the bone surface for computer-assisted surgery (CAS), this investigation reports the development and evaluation of intraoperative registration using 2D ultrasound (US) images. This approach employs automatic segmentation of the bone surface reflection from US images tagged with the 3D position to enable the application of CAS to minimally invasive procedures.

**Methods:** The US-based registration method was evaluated in comparison to point-based registration, which is the predominant method in current clinical use. The absolute accuracy of the US-based registration was determined using a phantom pelvis, with fiducial registration providing the ground truth. The relative accuracy was determined by an intraoperative study comparing the US registration to the point-based registration obtained as part of the HipNav<sup>TM</sup> experimental protocol.

**Results:** The phantom pelvis study demonstrated equivalent accuracy between point- and US-based registration under in vitro conditions. In the intraoperative study, the US-based registration was sufficiently consistent with the point-based registration to warrant larger-scale clinical trials of this non-invasive registration method.

**Conclusion:** Ultrasound-based registration eliminates the need for physical contact with the bone surface as in point-based registration. As a result, non-invasive registration could fully unlock the potential of computer-assisted surgery, enabling development of the next generation of minimally invasive surgical procedures. *Comp Aid Surg* 8:1-16 (2003). ©2003 CAS Journal, LLC

---

**Key words:** ultrasound, non-invasive registration, surgical navigation

---

### INTRODUCTION

Intraoperative registration is one of the key enabling steps of computer-assisted surgery (CAS). The registration determines the precise spatial relationship between the anatomical structures in the preoperative images and their corresponding locations within the operative field. The deter-

mined spatial relationship between the anatomy and the instruments can then be used to guide the surgical procedure according to the preoperative planning.<sup>1</sup> This allows surgical procedures to be performed not only more accurately but also less invasively by reducing the amount of dissection or

---

Received May 23, 2002; accepted March 5, 2003

Address correspondence/reprint requests to: Devin V. Amin 5914 Walnut St Apt 101, Pittsburgh, PA 15232; Telephone: (412) 361-5776; Fax: (412) 268-6436; E-mail: da2q@andrew.cmu.edu

©2003 CAS Journal, LLC

exposure necessary for the surgeon to become oriented to the anatomic landmarks. The registration is often based on the 3D shape of the bone surface present in the preoperative computed tomography (CT) images, since the rigid nature of bone tissue ensures that it will not deform or change shape between the time of image acquisition and the surgical procedure.<sup>2-4</sup> The 3D shape of the bone surface is segmented from the preoperative CT image to produce a triangular mesh or surface model that facilitates intraoperative registration.

The predominant shape-based method of intraoperative registration in current clinical use is point-based registration, which uses a position-sensing probe to contact the bone surface either percutaneously (directly puncturing the skin) for superficial regions or through the surgical incision for deeper regions. An alternative method is ultrasound-based registration, which is less invasive in that the sensor does not require direct contact with the bone surface.<sup>1,5-12</sup> An ultrasound probe coupled to a 3D position sensor could provide the intraoperative registration data for surgical procedures that involve limited access to the bone surface, such as arthroscopic procedures.<sup>12-14</sup> In fact, this facilitates one of the primary advantages of computer-assisted surgical techniques—the ability to reduce the amount of surgical exposure necessary to perform a given procedure.<sup>15-18</sup>

### Overview of Ultrasound Registration

Ultrasound (US) imaging can provide precise spatial information on the location of the bone surface intraoperatively. This information can be used to relate the preoperative planning to the intraoperative surgical actions. Prior to the surgical procedure, the preoperative plans are developed based on the surface model constructed from the preoperative CT scan.<sup>2,18</sup> Registering the US images to the surface model determines the intraoperative location of the relevant anatomy, allowing guidance of the intraoperative actions from the preoperative plans. To begin this registration procedure, the approximate position of a set of superficial anatomic landmarks can be collected without penetrating the skin surface. These anatomic landmark positions are used to define the starting point of the registration and also to specify which region of each US image is most likely to contain the bone surface reflection.<sup>1</sup>

Once the initial registration estimate has been defined, a set of 2D US images are obtained. The intraoperative 3D position sensor (Optotrak, Northern Digital, Inc., Waterloo, Ontario, Canada)

measures the position and orientation of an optical tracking target attached to the US probe. To relate the position and orientation of the position sensor attached to the US probe to the location of the US image, a calibration routine is required.<sup>19</sup> The location of each US image is measured relative to a dynamic reference base (DRB) that is rigidly fixed to the bone. This enables measurement of the location of each 2D US image in the 3D intraoperative coordinate system (see Figure 1).

A model of the US image formation process is used to locate the bone surface reflection within each US image. These regions of the ultrasound images are used to form a 3D distribution of image intensities which are then registered to the surface model from the preoperative CT using a surface-based registration algorithm.<sup>1</sup> Thus, without directly contacting the bone surface, ultrasound can be used to determine the intraoperative registration.<sup>8-11,13,14,20</sup> This allows guidance from the surgical navigation system to supplement the surgeon's visual orientation and enable the development of less invasive and more accurate surgical techniques.<sup>4,15-18,21-25</sup>

### Review of Prior Work

Previously reported research on ultrasound registration of the bone surface used manual segmentation of the bone surface from each US image.<sup>13,14</sup> Other applications of US registration us-



Fig. 1. The goal of US registration is to localize a set of 2D US image planes relative to the surface model of the pelvis obtained from a preoperative CT.

ing manually extracted surfaces include the registration of the cerebral ventricles for intracranial surgical procedures.<sup>9,10</sup> An automatic US registration method was developed for registration of soft-tissue structures such as the prostate and also applied to registration of the pelvic surface.<sup>12</sup> This method used a watershed-based image-processing technique to locate the tissue boundaries in the US images. The primary difference in this method, as compared to prior work targeted at the registration of the bone surface, was the use of an elastic rather than a rigid registration method. The registration of soft-tissue structures requires the use of elastic registration techniques that have additional degrees of freedom to accommodate the deformations in shape between the preoperative CT images and the intraoperative US images.

The manual segmentation of the bone surface reflection from the ultrasound images during the operative procedure typically requires an additional 20 min of operating room (OR) time.<sup>13</sup> In contrast, the currently used point-based registration techniques require less than 2 min of OR time. Thus, automatic segmentation methods were deemed necessary for the widespread application of US registration. The registration method presented in this paper eliminates the need to manually segment bone surface reflection from the US images. As a result, automatic US registration of the bone surface can now be accomplished with OR time requirements that are similar to currently used point-based registration methods.

### Physics of Ultrasound Image Formation

Medical ultrasound images, like visible light images, are produced by the reflection of energy from the object being imaged. Ultrasonic imaging systems transmit brief bursts or pulses of acoustic energy and record the time delay between the emission of the energy and the reception of successive reflected wave fronts. These pulses contain only a few complete cycles of the US signal, thus they are short in terms of their length in space (e.g., a 10-MHz signal that spans two full cycles has an overall length of 0.3 mm). The amount of energy reflected at the boundary of tissue types is described by the reflection coefficient  $R$ , where  $Z_1$  and  $Z_2$  are the acoustic impedance of the tissue before and after the boundary, respectively:

$$R = \left( \frac{z_2 - z_1}{z_2 + z_1} \right)^2 \quad (1)$$

The depth at which a given reflection occurs can be calculated from the average speed of ultrasound propagation through soft tissues and the time lapse until the reception of the reflected energy, as the approximate propagation velocity for soft tissue is 1500 m/s.<sup>26,27</sup> To form the 2D US image, the magnitude of the reflection is reported as the image intensity and the time lapse is reported as the depth or vertical position of the image intensity on the screen. To maximize the intensity of the bone surface reflection in the US image, the US probe is aimed as perpendicular or normal to the bone surface as possible to obtain a specular reflection from the interface between the bone and the soft tissue.

### Bone Shadow Region: Occlusion

Ultrasound images can exhibit the property of occlusion. A large transition in acoustic impedance will reflect the majority of the propagating ultrasound energy (i.e., the reflection coefficient approaches 1 if  $Z_2 \gg Z_1$ ) and leave very little US energy to propagate and image deeper structures. An area of occlusion in a US image, also called the shadow region, is typically a region of low intensity extending from the reflecting boundary to the bottom of the image. The transition in acoustic impedance between the soft tissue and the bone is so great that this interface essentially acts as a complete reflector of the propagating US energy.<sup>28,29</sup> Any anatomic structures deeper than the bone surface are occluded. The presence of the shadow region behind the bone is one of the most consistent features of US images of the bone surface (see Figure 2). This is in contrast to the CT imaging modality, which does not exhibit occlusion since it is based on the transmission of X-ray energy through the tissue (see Figure 3).

### Bone Surface Reflection / Angle of Incidence

The reception of the US reflection from the bone surface is very dependent upon the angle of incidence (i.e., the angle between the surface normal and the US propagation direction) at which the propagating US energy strikes the transition in acoustic impedance. If the angle of incidence is nearly zero, most of the energy is reflected back to the US probe, resulting in a very high-intensity bone surface reflection in the US image. As the angle of incidence increases, the amount of energy reflected back to the US probe decreases. At 45° or more, the majority of the reflected energy will not return to the US probe to be detected and

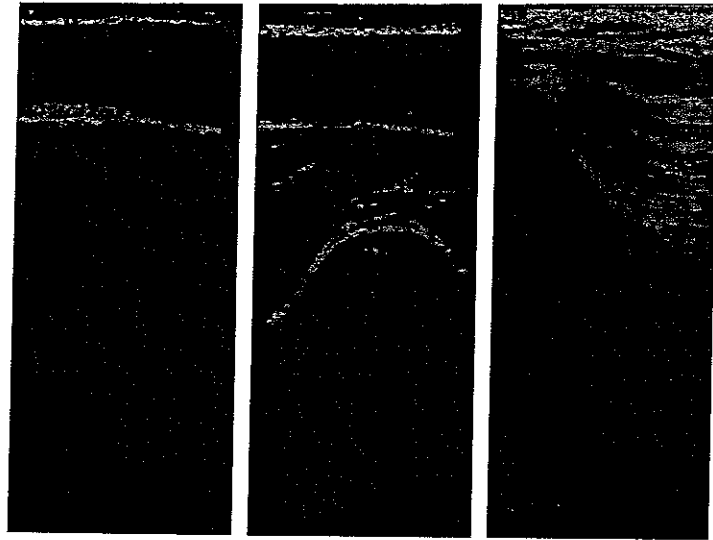


Fig. 2. Three US images demonstrating the angle of incidence phenomena. Left: medial condyle of the femur. Center: diaphysis of the femur. Right: iliac wing of the pelvis. A much stronger bone surface reflection is obtained in the first and second images, where the angle of incidence is close to zero, as opposed to the right image, where the angle of incidence is approximately  $45^\circ$ .

the bone surface reflection will not be visible in the US image (see Figure 2).<sup>26</sup>

The true angle of incidence may not always be apparent in the US image, as the surfaces being imaged are three-dimensional and the surface normals could be oriented out of the US imaging plane. To a large extent, the surgeon can compensate for these phenomena by using the feedback from the US monitor and knowledge of the anatomy to aim the US probe to obtain the maximal intensity bone surface reflection.<sup>1,5-7</sup>

### INTENSITY-BASED SURFACE REGISTRATION METHOD

The physics of ultrasound image formation predict that the interface between the bone and the soft tissue in a US image will appear as a high-intensity bone surface reflection followed by a low-intensity shadow region that extends to the bottom of the image (i.e., the region of the image opposite the US probe). This property, however, may not always be valid due to factors such as the angle of incidence (the US propagation direction relative to the bone surface normal) and the dependence of the image intensity on the tissue depth. Therefore, segmentation of the bone surface from the US image is a difficult task if performed using only the information available in the image itself.

However, combining a spatial prior from the initial registration estimate with the information

from the US image achieves automatic registration without manual segmentation. The three sources of information are the spatial prior based on a set of anatomic landmarks; the bone surface reflection indicated by the US image intensity; and the bone shadow region indicated by a directional edge detector. Rather than an explicit segmentation of the bone surface as a contour, a set of 2D regions likely to contain the bone surface reflection is obtained. During the registration, this region-based segmentation is refined to retain the data that is most consistent with the 3D shape of

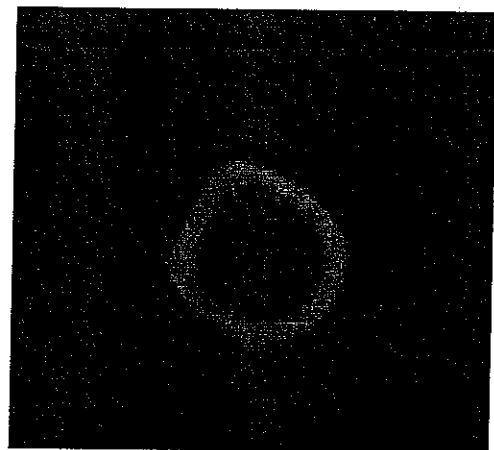


Fig. 3. Axial CT image of the femur showing the interior margins of the bone as it does not exhibit the phenomena of occlusion.

the surface model, essentially solving the final segmentation and registration steps simultaneously. In this manner, the final decision as to which pixels represent the bone surface is deferred from the US image processing stage to the registration stage where additional constraints are available. Thus, using multiple sources of information avoids the difficulty of segmenting the bone surface at the US image level. This method combines aspects of intensity-based registration algorithms, such as correlation and mutual information, with surface-based registration algorithms.

### Computation of the Registration Transform

The iterative closest points (ICP) algorithm provides an efficient method for computing the registration transform.<sup>30</sup> The ICP algorithm determines the optimum rigid registration in terms of a rotation ( $R$ ) and translation ( $T$ ) between the set of 3D points collected with the intraoperative US images (measured dataset  $U$ , where  $U = \{u_k\}$ , the set of all bone surface pixels in the US images) and the CT surface model,  $S$ . This rigid transform has six degrees of freedom; three for rotation and three for translation.

The ICP registration algorithm consists of three steps at each iteration. In the first step, each 3D point  $u_k$  of the intraoperative measurements of the bone surface location from the US images is paired with the closest point on the surface model,  $S$ . The closed-form registration solution requires a set of corresponding points in the two coordinate systems to be registered. In place of the true correspondence, which is unknown *a priori*, the Euclidean distance metric is used by the closest-point operator  $E$  to pair each intraoperative point  $u_{[i]}$  to the closest point on the surface model. Once the correspondence has been assigned using the closest-point operator, every element  $c_{[i]}$  is the closest corresponding point in  $S$  to the point  $u_{[i]}$ .

$$c_k = E(u_k, S) \quad (2)$$

The second step computes the registration update transform using a closed-form solution for the absolute orientation outlined below. This solution minimizes the sum of the squared distance between the paired points:

$$\{R_u, T_u\} = \arg \min \sum \|c_k - (R \cdot u_k + T)\| \quad (3)$$

The third step is to apply the registration update transform to the intraoperative points to move them into a closer alignment with the preoperative points. Typically, after iterating this method, the residual distance between each pair of points  $u_{[i]}$  and  $c_{[i]}$  will converge to an error below a pre-set threshold and terminate the registration process. The registration transform associated with the lowest sum of the residual distances is then reported as the final registration solution. This registration solution is the spatial relationship between the CT coordinate system containing the preoperative plans and the intraoperative coordinate system allowing guidance from the preoperative plans to be applied to the intraoperative actions.

### Closed-Form Least Squares Solution of Absolute Orientation

The second step above, equation (3), is computed using the closed-form solution for absolute orientation that was proposed by Horn and later incorporated into the ICP registration method by Besl and McKay.<sup>30,31</sup> The original derivation of this solution uses quaternions to represent the rotational component. Quaternions represent rotations in a compact format (i.e., four element vectors) and have attractive properties such as the ease of maintaining an orthonormal basis throughout the absolute orientation computation. Rotation can also be represented in terms of the more common homogeneous matrix (nine element,  $3 \times 3$  matrix), although at the expense of a more complicated derivation due to the difficulty of enforcing the orthonormality of the solution matrix.<sup>32</sup> In this work, the computation is performed with the quaternion approach and then the solution is converted into a homogeneous rotation matrix format.

The solution for the absolute orientation begins with the formation of the  $3 \times 3$  cross covariance matrix,  $\Sigma_{uc}$ . The mean of the US,  $\vec{m}_u$ , and CT,  $\vec{m}_c$ , points is calculated and represented by a  $3 \times 1$  column vector. The  $3 \times 3$  matrix is then formed from the summation of the matrix product of each pair of 3D points from US,  $\vec{u}_k$ , and CT,  $\vec{c}_k$ , coordinate systems.

$$\Sigma_{uc} = \frac{1}{N} \sum_{k=1}^N (\vec{u}_k \cdot \vec{c}_k^T) - \vec{m}_u \cdot \vec{m}_c^T \quad (4)$$

The  $3 \times 3$  anti-symmetric matrix  $A$  is formed from the cross-covariance matrix ( $\Sigma_{uc}$ ) and the ele-

ments of  $A_{ij}$  are used to form the  $3 \times 1$  column vector  $v$ :

$$A_{ij} = \left( \sum_{uc} - \sum_{uc}^T \right)_{ij} \quad (5)$$

$$v = [A_{23} \ A_{31} \ A_{12}]^T \quad (6)$$

Then the matrix  $Q$ , a  $4 \times 4$  symmetric matrix, is formed from the covariance matrix ( $\Sigma_{uc}$ ) and the column vector  $v$ , where  $\text{tr}()$  signifies the trace operator of the matrix:

$$Q(\Sigma_{uc}) = \begin{bmatrix} \text{tr}(\Sigma_{uc}) & v^T \\ v & \Sigma_{uc} + \Sigma_{uc}^T - \text{tr}(\Sigma_{uc})I_{3 \times 3} \end{bmatrix} \quad (7)$$

The eigenvector decomposition of the matrix  $Q$  yields the optimal rotation between the two point sets. The eigenvector corresponding to the maximum eigenvalue of  $Q$  is a unit quaternion corresponding to the optimal rotation:

$$\tilde{q}_R = [q_0 \ q_1 \ q_2 \ q_3]^T \quad (8)$$

The quaternion representation of the optimal rotation is then converted to the homogenous matrix representation  $R$  and applied to the intraoperatively measured points  $\{u_i\}$  to bring them closer to the surface model. The optimal translation between the two datasets is now simply the vector defined by the difference between the mean of the two datasets:

$$T = \tilde{m}_c - R(\tilde{q}_R) \cdot \tilde{m}_u \quad (9)$$

### Termination of the Registration Process

In this manner, the ICP algorithm registers a set of intraoperative 3D points to a surface model by using the closest-point operator to assign the correspondence and the closed-form computation of the absolute orientation to compute the registration update transform. This process is iterated until one of the termination conditions is satisfied. The termination conditions are that the parameters of the registration update transform are all less than a preset threshold (i.e., the theoretical accuracy of the registration), or that the incremental decrease of the residual error is less than a preset threshold. Also, a maximum number of iterations is specified as a termination condition, although exceeding the maximum iteration limit is more indicative of registration failure than determination of a successful solution.<sup>2</sup> The ICP algorithm has been demonstrated to converge to the correct registration for most 3D objects when a suitable initial registration estimate is available.<sup>30</sup>

### Incorporating Prior Information into the ICP Registration

The objective function of the ICP algorithm seeks to find the rotation and translation that minimize the sum of the squared distance between the US bone surface points,  $U$ , and the CT surface model,  $S$ . The formulation of the ICP algorithm allows for a weight to be applied to each of the points being registered to the surface model. This weight can incorporate the prior information as to the likelihood that a given US pixel represents the location of the bone surface. This prior information is composed of three components: the spatial prior based on the current registration estimate ( $W_{IE}$ ); the intensity prior indicating the bone surface reflection ( $W_{INT}$ ); and the edge prior indicating the boundary of the bone shadow region ( $W_{EDGE}$ ). The composite weight term  $w_i$  is defined as the product of these terms:

$$w_i = W_{IE} \cdot W_{INT} \cdot W_{EDGE} \quad (10)$$

The product of these three components forms the weight vector ( $w_i$ ) and represents the likelihood that a given pixel of the US image represents the bone surface. This allows the bone surface reflection region to be segmented from the US image without making an explicit decision on the location of the bone surface. The addition of the weight function to the ICP registration equation yields the ultrasound-to-surface-model registration equation:

$$(R_s, T_s) = \arg \min_{R, T} \sum_k w_k \|c_k - (R \cdot u_k + T)\|^2 \quad (11)$$

### Characterization of the Three Sources of Prior Information

Each of the three coefficient terms used in the weights  $w_i$  considered alone would not be sufficiently reliable to segment the bone surface reflection region from the US image. However, the errors and biases of the three terms differ considerably, and when the combination of three sources of partial information is used, they enable automatic segmentation of the bone surface reflection region from the US image.<sup>1</sup>

#### 1. The spatial prior

The first component of the weight vector is the spatial prior,  $W_{IE}$ , based on the approximate locations of a set of anatomic landmarks identified by the surgeon. This orienting information provides an approximate location as to where the

bone surface is located within the ultrasound image. Regions of the ultrasound image that are distant from the initial estimate of the bone surface location are unlikely to contain the bone surface reflection, and are thus excluded from the registration process.

The computation of the spatial prior  $W_{IE}$  is based on the representation of the distance from the bone surface in the CT image volume. The 3D volumetric representation of the distance from the bone surface,  $BD(X)$ , can be computed by applying the Gaussian kernel at each voxel of the CT that has been extracted as the bone surface during the construction of the surface model.<sup>1,33</sup> The bone surface distance volume is the same size as the CT and can be computed preoperatively along with the construction of the surface model. The spatial prior information corresponding to each 2D US image is extracted using the current registration estimate to specify the location of the US image within the bone surface distance volume.

$$BD(X) = \sum_{k \in BS} G(X - X_k) \quad (12)$$

where  $G$  is a 3D Gaussian kernel applied at the 3D point  $\xi$ , ( $\xi = [\xi_x \ \xi_y \ \xi_z]$ ), and sigma squared,  $\sigma^2$ , is the specified variance of the kernel.

$$G(\xi) = \frac{1}{\sqrt{2\pi\sigma^2}} e^{-\frac{\xi_x^2 + \xi_y^2 + \xi_z^2}{2\sigma^2}} \quad (13)$$

This computation of the 3D spatial prior information using the bone surface distance volume can be approximated by first extracting a 2D slice from the original CT volume that corresponds to the US image in the location specified by the current registration estimate. The 2D region of CT data is then processed to recover the bone surface that would encounter the propagating US energy. The CT bone surface is then convolved with a 2D Gaussian kernel to obtain the spatial prior information in a 2D format that can be applied to the US image. This method does not fully take into account the 3D shape of the object, and thus is only an approximation of the spatial prior provided by the bone surface distance volume method. The advantage is that it simplifies the preprocessing stage by eliminating the need to produce and store the bone surface distance volume, reducing the memory requirements of the algorithm.

The size or support of the convolution kernel is related to the expected uncertainty of the

initial registration estimate. Experimental and simulation studies show that the anatomic landmarks can be collected with less than 20 mm error, giving confidence limits on the parameters of the initial estimate of 20 mm translation and 12° of rotation for an object the size of an adult pelvis. Thus, the size of the bone surface reflection region is directly related to the expected accuracy of the initial estimate of the registration. For the example shown in Figures 4 and 5, the support of the convolution kernel was chosen to reflect the translational uncertainty of the registration estimate, 20 mm. Therefore, the span of the bone surface reflection region would be approximately 40 mm in the axial direction.

The approach described above recalculates the spatial prior information at each iteration of the registration using the current registration estimate. As the current registration estimate becomes more accurate, the size of the spatial prior region could be reduced by using only the spatial prior region that corresponds to a higher iso-intensity contour. The iso-intensity level is increased in proportion to the residual error at each iteration. However, if the computational resources are limited, then the bone surface region from the initial estimate may be used throughout the registration process rather than being recomputed at each iteration. The validity of this approximation is dependent upon the accuracy of the initial estimate.

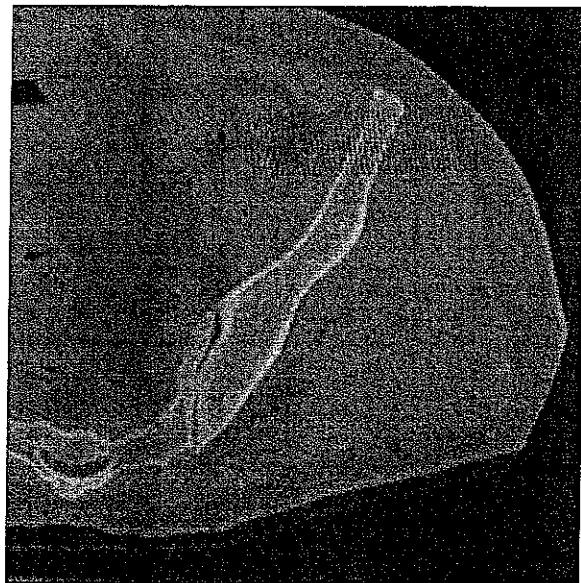


Fig. 4. CT image with highlighted rectangular region corresponding to US image. During registration, the location of a given US image within the CT volume can be computed.

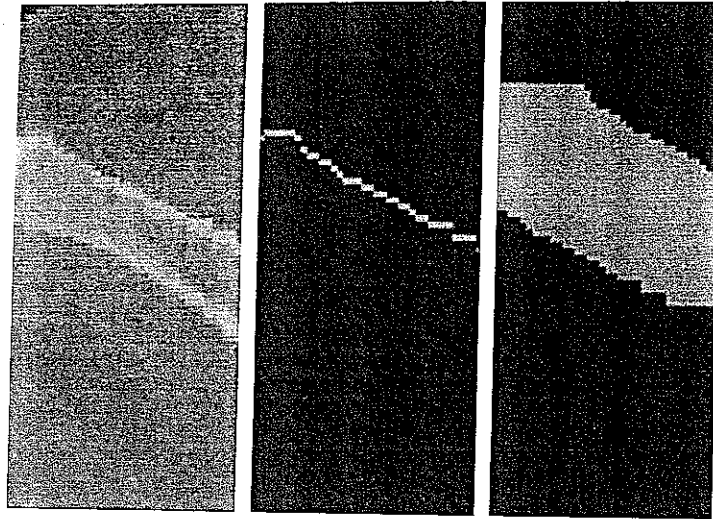


Fig. 5. Left: CT cross-section corresponding to a given US image. Center: Bone surface from CT image. Right: Initial estimate of bone surface region

### 2. The intensity prior

The image intensity of the bone surface in the US image is expected to be a high value due to the large transition in acoustic impedance between soft tissue and bone. Therefore, in the absence of any other information, the pixel intensity of the ultrasound image can be used to estimate the likelihood that a given pixel represents the bone surface reflection. This expectation is valid provided that the angle of incidence is within approximately  $20^\circ$  of the surface normal. The various phenomena and artifacts of US imaging may cause many non-bone surface regions of the US image to have equivalent or higher intensity than the bone surface. Thus, image intensity information alone would be insufficient to segment the bone surface reflection region from the US image.

### 3. The edge prior

The bone shadow region is one of the most invariant features available to locate the bone surface in the US images. The transition between the bone shadow region and the bone surface reflection can be located with a directional edge detector (see Figures 6 and 7). The directional edge detector propagates upward along each column. When a pixel intensity higher than an empirically based bone surface threshold is encountered, that pixel is set to one and all other pixels in the column are set to zero. This process implicitly assumes that each column of the US image contains at least one pixel on the bone surface, but this assumption may not be true for certain viewing

directions. Therefore, the surgeon chooses the viewing directions so that the bone surface spans the majority of the US image.

To ensure that the edge detector region captures the entirety of the bone surface reflection, which typically spans 1–2 mm in the axial direction of the US image, the directional edge output is blurred with a Gaussian kernel ( $\sigma = 2$  mm). The size of this kernel is relatively large in comparison to the US pixel size of approximately 0.25 mm, yet small relative to the CT voxel size of 1 mm. The final output of the directional edge detector represents the likelihood that a given ultrasound pixel represents the bone surface based on the bone shadow phenomena.

## REGISTRATION STUDIES

Two experimental studies were conducted to validate the ultrasound registration method. The first study evaluated the absolute registration accuracy by using a plastic phantom pelvis and a set of four fiducial spheres. The use of fiducial-based registration allows precise evaluation of the US-based registration accuracy. Point-based registration, the predominant technique in clinical use, was also performed on the phantom pelvis and its accuracy was compared to that of the US-based registration under identical conditions and in reference to the fiducial-based ground-truth registration.

In the second study, intraoperative US registration was performed and compared to point-based registration of the same patient. In the in-



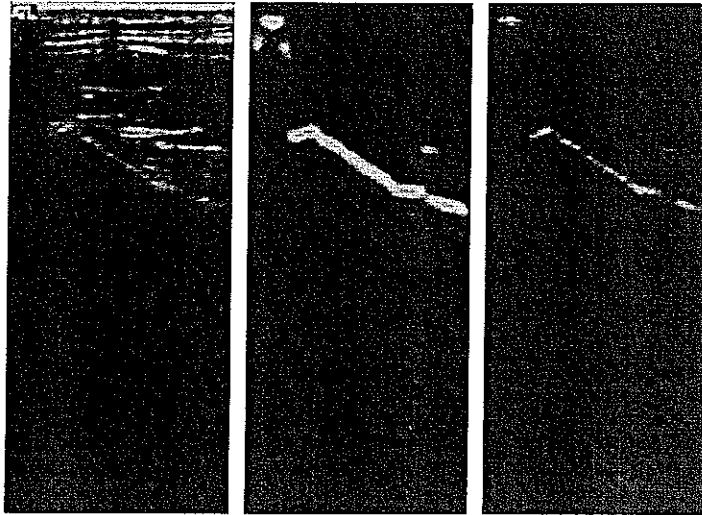


**Fig. 6.** The edge prior is applied to the US image to locate the bone surface reflection. Left: Original US image. Center: US image after directional edge detection and convolution with Gaussian kernel ( $\sigma = 2$  mm). Right: Center image multiplied by left image to select the bone surface reflection.

traoperative setting, fiducials are unavailable to provide the ground truth. Therefore, the accuracy of the US registration was assessed relative to point-based registration. This point-based registration method has been clinically tested and validated with the HipNav system on over 150 cases.<sup>15-18</sup>

### Registration of the Phantom Pelvis

A phantom registration study was conducted to evaluate the absolute accuracy of the US registra-

tion. In this study, fiducial-based registration provided the ground truth or true registration to evaluate the absolute accuracy. The phantom pelvis was submerged in a water transmission medium that served the function of the soft tissues that are superficial to the bone in the intraoperative setting. Four fiducial spheres were fixed to the pelvis. The location of these fiducials relative to the Optotrak® camera and in the CT volume could be accurately determined to provide a very accurate ground-truth registration to which

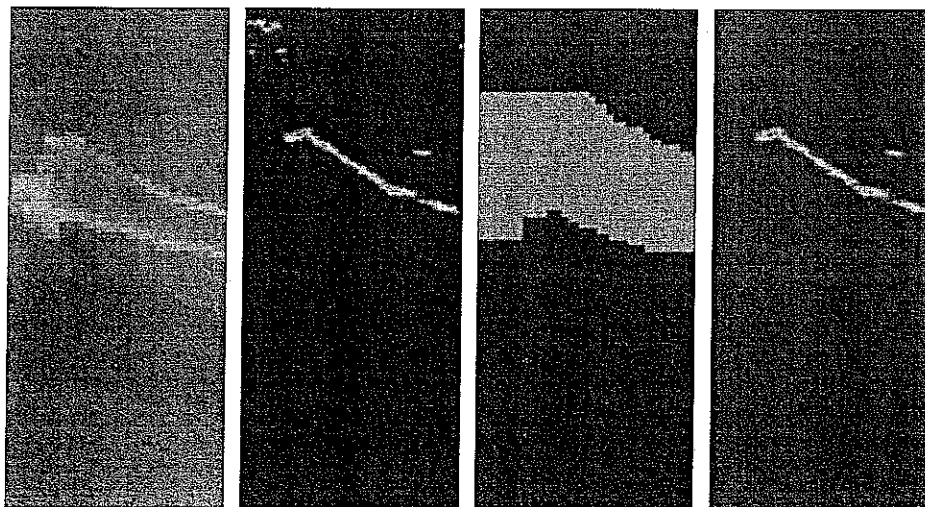


**Fig. 7.** The spatial prior is applied to the output of the edge prior to produce the final bone surface reflection region. From left to right: CT region corresponding to US image; US image following application of edge prior; spatial prior estimate of bone surface reflection as specified by anatomic landmark-based initial estimate; and final bone surface reflection region obtained by multiplication of edge and spatial prior information.

the US-based registration result could be compared.

For point-based registration, a set of surface points were collected from the surface of the phantom pelvis using a point probe in a manner that is typical for intraoperative registration (see Figure 8). This allowed the US registration to be compared directly to the point-based registration under identical conditions and in reference to fiducial-based ground truth. Point-based registration to a surface model is currently the predominant method in clinical use for intraoperative registration. Thus, equivalent accuracy relative to point-based registration would validate the accuracy of US registration.

### *Experimental Set-Up of the Phantom Registration*

In the phantom study, four fiducials were attached to the anatomic pelvis to provide a very accurate fiducial-based registration to which the US-based registration could be compared. In the context of medical image registration, a fiducial is any object that can be accurately localized in two different coordinate systems. A set of three or more fiducials can provide the spatial relationship or rigid transformation between two 3D coordinate systems. The fiducials used in this study were

aluminum spheres (12.7 mm in diameter). The physical locations of the four aluminum spheres were precisely measured on the pelvis model and in the CT image volume. A CT scan was obtained of the plastic pelvis including the four fiducial spheres. In the CT scan, the centers of the fiducial spheres were very accurately localized with software that determines the center of each of the fiducial spheres in the CT image volume. The 3D location of the sphere center in physical space was also accurately measured by the optical tracking system using an optically tracked probe fitted with a hollow cylindrical tip (inner diameter of the cylinder = 8.7 mm) calibrated to measure the center of the spherical fiducial. Measuring the location of these four fiducial spheres in both the CT and the intraoperative coordinate systems allows computation of the ground-truth registration.

The phantom pelvic model was submerged in water and an optically tracked dynamic reference base (DRB) was rigidly attached to the iliac wing with a custom fixation clamp (see Figure 9). All subsequent 3D position measurements in this study were collected relative to the DRB. This compensated for any motion of the pelvic model during data collection. For the data to be valid, the DRB must remain rigidly fixed to the pelvis throughout the data collection procedure. This

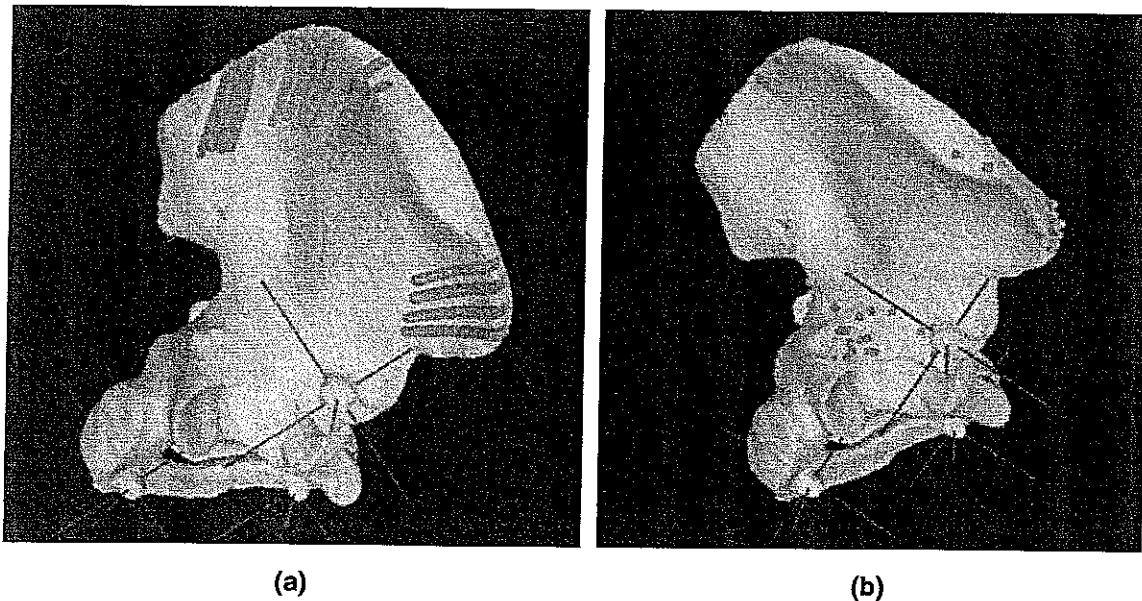


**Fig. 8.** US registration to a surface model of the phantom pelvis and point-based registration for comparison. a) US bone surface reflections are correctly registered to the surface model of the phantom pelvis b) Points collected from intraoperatively accessible regions of the pelvic surface are correctly registered to the surface model. In both figures the initial registration landmarks (obtained by a random perturbation of the fiducial spheres location) are indicated by the three coordinate axes

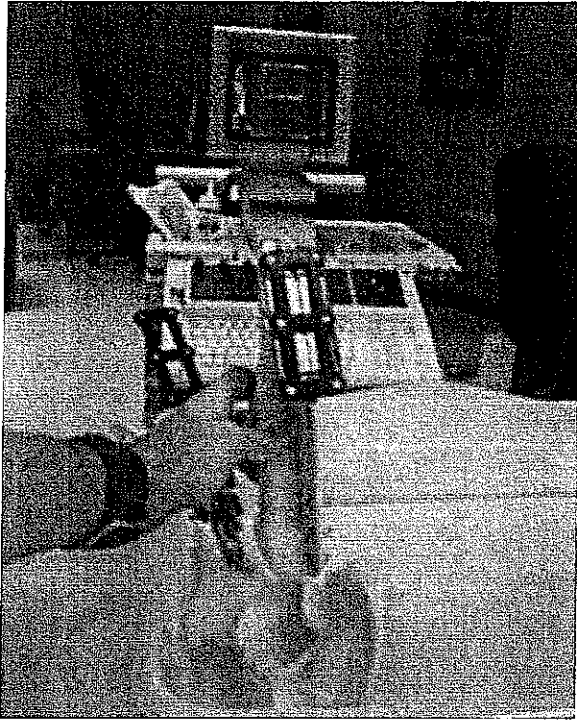


**Fig. 9.** Experimental set-up consisting of a dynamic reference base in the form of an optical tracker attached to the iliac wing of the phantom pelvis via a rigid fixation clamp and the US probe fitted with a calibrated molded shell and optical tracker to measure the 3D position of the US image.

was verified by ensuring that the location of the fiducial spheres relative to the DRB was the same (i.e., within the Optotrak precision of 0.3 mm) both before and after ultrasound data collection.

The US images were digitized by video capture off the US machine (Siemens Sonoline Elegra) and tagged with the respective 3D position and orientation of the US probe (linear array transducer, 7.5 MHz). The choice of US machine should not affect the results of the registration provided that an image of similar quality is obtained from the bone surface. The synchronization of the collection of the Optotrak position and the US image was provided by acquiring the 3D position first and then immediately capturing the video image, although some time delay is inevitable and this is one possible source of error. To relate the measured position of the US probe to the relative position of the US image, the spatial relationship of the US image plane must be calibrated relative to the optical tracker attached to the US probe.<sup>19,34</sup> The accuracy of this calibration inherently affects the overall US registration accuracy. This calibration was accomplished by re-

peatedly collecting an image containing a known point in physical space. The complete details of this calibration method are described in a separate publication.<sup>19</sup>

In contrast to the US images of the patient's pelvic surface obtained intraoperatively, collecting the US images in a water medium simplified the segmentation of the bone surface reflection. Collection of US images in a water medium provides an homogeneous reflection interface at the bone surface. The lack of artifacts from soft tissue (e.g., fat and muscle) overlying the bone surface, such as occur with intraoperative US images, greatly simplified the extraction of the bone surface from the US images of the phantom pelvis.

Using the location of the calibrated US probe relative to the DRB, these bone surface reflections were converted to a set of 3D points and registered to the surface model of the phantom pelvis (see Figure 8). A total of 50 US images were collected over the iliac wing region of the pelvis. The anatomic landmark-based initial registration was used as the starting point for the registration process. Ten registration trials were conducted by selecting a random subset of 20 US images and registering them to the surface model derived from the CT.

For purposes of comparing US-based registration to point-based registration, 100 points were collected with the 3D position-sensing probe from the surgically accessible regions of the pelvic bone surface. Ten registration trials were conducted by choosing a random subset of 46 surface points (the typical number used for intraoperative registration) and registering them to the surface model of the phantom pelvis. The absolute accuracy of the point-based registration was evaluated in comparison to the fiducial-based registration. The accuracy of US registration relative to that of the well-established point-based registration was then obtained using the fiducial-based registration to provide an objective basis for comparison.

### *Results of the Phantom Registration*

The registration results in Table 1 demonstrate the ability of ultrasound registration to accurately determine the location of the phantom pelvis with an average error of less than 0.5 mm of translation and 0.5° of rotation in each axis. The location results are given in terms of six registration parameters (three for translation and three for rotation). Over the set of ten US registration trials, the maximum registration error, as compared to the fiducial-based ground truth, was less than 1

**Table 1. Phantom Pelvis Registration Study Results: Maximum and RMS Error for US- and Point-Based Registration of the Phantom Pelvis Relative to Fiducial-Based Registration**

		Translational error (for each axis in mm)			Rotational error (for each axis in °)			Avg. trans.	Avg. rot.
		I <sub>x</sub>	I <sub>y</sub>	I <sub>z</sub>	R <sub>x</sub>	R <sub>y</sub>	R <sub>z</sub>	I	R
US-based	Maximum error	0.29	0.31	0.76	0.22	1.04	0.26	0.45	0.42
	RMS error	0.64	0.21	0.32	0.10	0.54	0.15	0.39	0.26
Point-based	Maximum error	0.19	1.11	1.11	0.42	0.65	0.44	0.80	0.50
	RMS error	0.10	0.64	0.55	0.24	0.37	0.28	0.43	0.29

mm and less than 2° in each axis. In fact, out of ten trials, only one had a rotational error greater than 1°. The results for the point-based registration were similar, with less than 2 mm and 1° in each axis.

## DISCUSSION

The US- and point-based registration methods demonstrated very similar accuracy in comparison to the fiducial-based registration ground truth. The conclusion from these results is that, under controlled conditions, the accuracy of the US-based registration is equivalent to the point-based registration method. Successful registration of the phantom pelvis demonstrated the ability of the ultrasound-based registration method to determine the location of a 3D object using data from the calibrated US probe. This validated the concept of non-invasive registration and demonstrated its potential for intraoperative registration.

The benefit of US-based registration is that it maintains the accuracy of point-based registration while enabling non-invasive surface-based registration. This allows increased access to the bone surface for the collection of registration information, whereas point-based registration is restricted to collecting registration data through the surgical incision or percutaneously for superficial regions of the bone surface.

### Intraoperative Registration

The accuracy of US-based registration was evaluated in comparison to a clinically validated point-based registration method under intraoperative conditions. Ultrasound images were collected from a patient under sterile conditions after the placement of a DRB on the iliac wing of the patient's pelvis to establish the intraoperative coordinate system (see Figures 10 and 11). The point-based registration was performed as part of the standard HipNav™ protocol and used to determine the relative accuracy of US registration,

since fiducial-based registration was unavailable intraoperatively.

### Experimental Setup of the Intraoperative Registration

The experimental protocol describing the use of intraoperative ultrasound was submitted and approved by the institutional review board of UPMC Shadyside Hospital. A patient scheduled for total hip replacement was selected, and consent for the use of intraoperative US was obtained in conjunction with the standard consent for the HipNav™ protocol.<sup>1</sup> To begin the procedure, the patient was prepared and draped for hip replacement surgery. In accordance with standard HipNav™ protocol, the DRB was attached to the iliac wing with a custom fixation clamp.<sup>15-18</sup> Once the DRB was placed, three initial registration landmark points were collected, then 100 US images

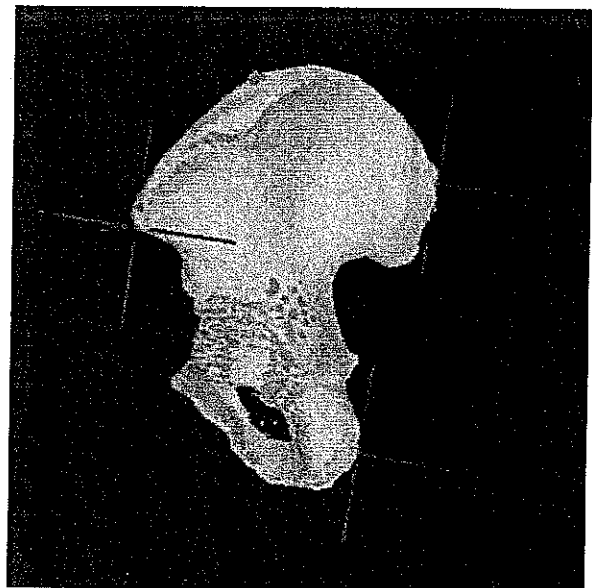


**Fig. 10.** Results of intraoperative point-based registration: the 3D points collected from the pelvic bone surface are registered to the patient-specific surface model from the preoperative CT.

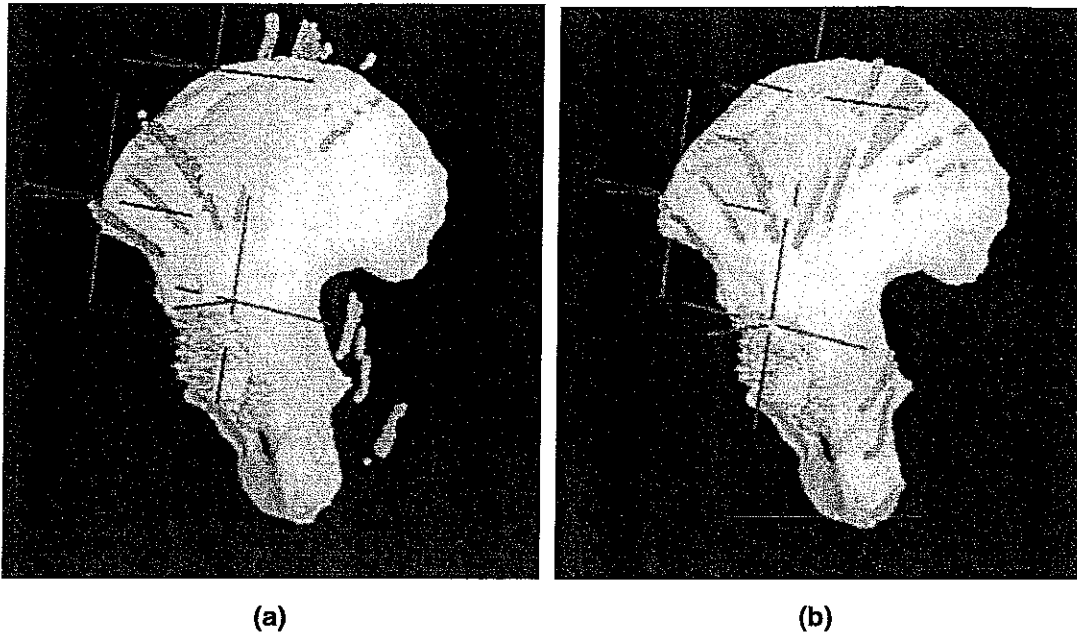


**Fig. 11.** Intraoperative US bone surface reflection regions shown before (a) and after (b) registration to the surface model of the patient's pelvis

of the pelvic bone surface were collected by the surgeon using sterile procedure. There is a certain amount of training and familiarity required for the successful implementation of any new technology, but in the case of obtaining US images of the bone surface the learning process is rapid, since visual feedback is immediately available. The surgeon aimed the US probe approximately normal or perpendicular to the bone surface to obtain a strong bone surface reflection prior to collecting each US image. The probe is positioned such that the bone surface reflection spans the majority of the image to maximize the yield of each image collected. The real-time nature of US imaging provides immediate visual feedback to the surgeon to confirm that the probe is aimed appropriately prior to the collection of each image.

Ultrasound images were collected predominantly over the iliac crest region, with a few images of the ischial tuberosity and sciatic notch areas. The total OR time required to collect 100 US images of the bone surface was approximately 15 min. For routine US registration, 30 US images would be sufficient, requiring less than 5 min of OR time for data collection. The US probe was then removed from the sterile operating field and the surgical procedure continued according to the standard HipNav™ protocol.

The US registration trials were performed following the completion of the operation. In each

registration trial, 30 US images were selected at random from the original 100 images and registered to the surface model of the patient's pelvis. A set of 10 registration trials were conducted by choosing a different subset of 30 images for each trial. In the intraoperative study, fiducials were not available to provide the ground truth. Therefore, the point-based registration from the HipNav™ protocol was used as the ground truth to which the results of the US-based registration trials were compared.

#### *Results of the Intraoperative Registration*

Over the 10 registration trials, the maximum difference in translation between US-based registration and point-based registration was 2.07 mm, with a maximum rotational difference of 1.58 degrees (see Table 2). The computation time of the US-based registration solution was approximately 90 s for US-based registration and 10 s for point-based registration (on an SGI Octane workstation)

#### *Discussion*

The accuracy of the intraoperative ultrasound-based registration method was demonstrated to be comparable to that of point registration (within 3 mm and 2°) over a series of ten registration trials. The effect of the learning curve on the collection of intraoperative US images must be taken

Table 2. Intraoperative US Registration Study Results: Maximum and RMS Error for US-Based Registration Relative to Intraoperative Point-Based Registration

		Translational error (for each axis in mm)			Rotational error (for each axis in °)			Avg. trans. I	Avg. rot. R
		I <sub>x</sub>	I <sub>y</sub>	I <sub>z</sub>	R <sub>x</sub>	R <sub>y</sub>	R <sub>z</sub>		
US-based	Maximum error	1.98	1.76	2.06	1.58	0.72	0.39	1.94	0.90
	RMS error	1.24	0.99	1.59	1.10	0.45	0.21	1.27	0.59

into account. As surgeons gain more experience with collecting US images intraoperatively, the overall accuracy of the registration solution would be expected to increase and become more consistent across individual patients. The comparable accuracy of US registration relative to point-based registration demonstrated by these results validates the use of ultrasound registration for less invasive applications of computer-assisted surgery.

## CONCLUSION

Registration methods that utilize intraoperative imaging modalities often depend on segmentation of anatomic structures within the intraoperative images. The various noise, artifacts, and imaging phenomena of ultrasound make reliable segmentation of the bone surface difficult. The solution to this problem presented in this article avoids explicit segmentation of the bone surface at the image level, and instead combines three sources of information to perform a region-based extraction of the bone surface reflection. The final segmentation process is performed during the registration process: As the registration estimate converges to the solution, the 3D shape of the object is used to drive the final segmentation process.

Several surgical procedures, such as the percutaneous placement of ilio-sacral screws for the treatment of pelvic ring fractures, would be excellent candidates for the clinical application of this non-invasive registration method.<sup>13 14</sup> However, the ultimate benefit of this work may be realized through its application to more common minimally invasive orthopedic procedures such as arthroscopic anterior cruciate ligament repair. These procedures make the use of point-based registration difficult or even impossible due to the limited surgical access to the bone surface, and are currently dependent on fiducial-based registration methods that require an additional implantation procedure prior to the acquisition of the preoperative CT scan.

The registration method described here is based on ultrasound imaging that is widely avail-

able in most hospitals and is often used for diagnosis and guidance in the OR. The advent of ultrasound registration will reduce the invasiveness of current computer-assisted surgical techniques and ultimately enable surgeons and researchers to develop novel surgical procedures to treat a variety of debilitating conditions.

## ACKNOWLEDGMENTS

We gratefully acknowledge support from the Medical Robotics and Computer Assisted Surgery Fellowship of the Shadyside Hospital Foundation.

## REFERENCES

1. Amin DV. Ultrasound Registration for Surgical Navigation. Doctoral thesis, Carnegie Mellon University, 2001.
2. Simon DA. Fast and accurate shape-based registration. Technical Report, CMU-RI-IR-96-45. Carnegie Mellon University, December 12, 1996.
3. Lunsford LD. A dedicated CT System for the stereotactic operating room. *Appl Neurophysiol* 1982;45: 374-378.
4. Macunias RJ, editor. *Interactive Image Guided Neurosurgery*. American Association of Neurological Surgeons, 1993.
5. Amin DV, Kanade I, DiGioia AM, Jaramaz B, Nikou C, LaBarca RS, Moody JE, Levison IJ, Cipriani JA. Direct registration of intraoperative ultrasound to preoperative CT for image guided surgery. In: *Proceedings of the Fifth Annual North American Program on Computer Assisted Orthopaedic Surgery (CAOS USA 2001)*, Pittsburgh, PA, July 2001. p 237.
6. Amin DV, Kanade I, DiGioia AM, Jaramaz B, Nikou C, LaBarca RS, Moody JE. Non-invasive ultrasound registration of the pelvic bone surface for THR. *Transactions of the 47th Annual Meeting of the Orthopaedic Research Society*, San Francisco, CA, 2001. Paper 1072.
7. Amin DV, Kanade I, DiGioia AM, Jaramaz B, Nikou C, LaBarca RS. Ultrasound based registration of the pelvic bone surface for surgical navigation. *Proceedings of the First International Conference on Computer Assisted Orthopedic Surgery*, Davos, Switzerland, February 2001. p 36.
8. Ault I, Siegel MW. Painless patient location using

- ultrasonic imaging In: Proceedings of the First Annual Symposium on Medical Robotics and Computer Assisted Surgery (MRCAS). Pittsburgh, Pennsylvania, 1994. p 74-81
9. Erbe H, Kriete A, Jödicke A, Deinsberger W, Böker D-K. 3D-ultrasonography and image matching for detection of brain shift during intracranial surgery In: Lemke HU, Vannier MW, Inamura K, Farman AG, editors: Computer Assisted Radiology. Proceedings of the International Symposium on Computer and Communication Systems for Image Guided Diagnosis and Therapy (CAR'96), Paris, June 1996. Amsterdam: Elsevier, 1996. p 225-230.
  10. Hata N, Suzuki M, Dohi I, et al. Registration of ultrasound echography for intraoperative use: A newly developed multiproperty method. Visualization in Biomedical Computing 1994. p 251-259.
  11. Jödicke A, Deinsberger W, Erbe H, Kriete A, Böker D-K. Intraoperative three-dimensional ultrasonography: An approach to register brain shift using multi-dimensional image processing. Minimally Invasive Neurosurgery 1998;41:13-19.
  12. Ionescu G, Lavallée S, Demongeot J. Automated registration of ultrasound with CT images: Application to computer assisted prostate radiotherapy and orthopedics. In: Taylor C, Colchester A, editors: Proceedings of the Second International Conference on Medical Image Computing and Computer-Assisted Intervention (MICCAI '99), Cambridge, UK, September 1999. Lecture Notes in Computer Science 1679. Berlin: Springer, 1999. p 768-777.
  13. Carrat L, Ionetti J, Lavallée S, Merloz P, Pittet L, Chirossel JP. Treatment of pelvic ring fractures: percutaneous computer assisted iliosacral screwing. In: Wells WM, Colchester A, Delp S, editors: Proceedings of the First International Conference on Medical Image Computing and Computer-Assisted Intervention (MICCAI '98), Cambridge, MA, October 1998. Lecture Notes in Computer Science 1496. Berlin: Springer, 1998. p 84-91.
  14. Carrat L, Tonetti J, Merloz P, Troccaz J. Percutaneous computer assisted iliosacral screwing: clinical validation. In: Delp SL, DiGioia AM, Jaramaz B, editors: Proceedings of the Third International Conference on Medical Image Computing and Computer Assisted Intervention (MICCAI 2000), Pittsburgh, PA, October 2000. Lecture Notes in Computer Science 1935. Berlin: Springer, 2000. p 1229-1237.
  15. DiGioia AM, Simon DA, Jaramaz B, Blackwell M, Morgan F, O'Toole R, Colgan B, Kischell E. HipNav: preoperative planning and intraoperative navigational guidance for acetabular implant placement in total hip replacement surgery. Proceedings of the Computer Assisted Orthopedic Surgery Symposium, Bern, Switzerland, 1995.
  16. DiGioia AM, Simon DA, Jaramaz B, Blackwell M, Morgan F, Colgan B. Intraoperative measurement of pelvic and acetabular component alignment using an image guided navigational tool. Proceedings of the 44th Annual Meeting of the Orthopaedic Research Society, New Orleans, Louisiana, 1998.
  17. DiGioia AM, Jaramaz B, Blackwell M, Simon DA, Morgan F, Moody JE, Nikou C, Colgan BD, Aston CA, LaBarca RS, Kischell E, Kanade T. Image guided navigation system to measure intraoperatively acetabular implant alignment. Clin Orthop Rel Res 1998;355:8-22.
  18. Simon DA, O'Toole RV, Blackwell MK, Morgan F, DiGioia AM, Kanade T. Accuracy validation in image-guided orthopedic surgery. Proceedings of the Second International Symposium on Medical Robotics and Computer Assisted Surgery (MRCAS '95), Baltimore, MD, November 1995. p 185-192.
  19. Amin DV, Kanade T, DiGioia AM, Jaramaz B, Nikou C, LaBarca RS, Moody JE. Calibration method for determining the physical location of the ultrasound image plane. Proceedings of the Fourth International Conference on Medical Image Computing and Computer-Assisted Intervention (MICCAI 2001), Utrecht, The Netherlands, October 2001.
  20. Barbe C, Troccaz J, Mazier B, Lavallée S. Using 2.5D echography in computer assisted spine surgery. IEEE Engineering in Medicine and Biology Society Proceedings, 1993. p 160-161.
  21. Troccaz J, Laieb N, Vassal P, Menguy Y, Cinquin P, Bolla M, Giraud JY. Patient set-up optimization for external conformal radiotherapy. Proceedings of the First International Symposium on Medical Robotics and Computer Assisted Surgery (MRCAS), Pittsburgh, PA, 1994. p 306-312.
  22. Maiuri F, Iaconetta G, Divitis OD. The role of intraoperative sonography in reducing invasiveness during surgery for spinal tumors. Minimally Invasive Neurosurg 1997;40:8-12.
  23. Leotta DF. Three-Dimensional Spatial Compounding of Ultrasound Images Acquired by Freehand Scanning: Volume Reconstruction of the Rotator Cuff. PhD thesis, University of Washington, 1998.
  24. Leksell L. Stereotaxis and Radiosurgery: An Operative System. Springfield, IL: Charles C Thomas Publisher, 1971.
  25. Nolte LP, Zamorano LJ, Zhaowei J, Wang Q, Langlotz F, Arm E, Visarius H. A novel approach to computer assisted spine surgery. Proceedings of the First International Symposium on Medical Robotics and Computer Assisted Surgery (MRCAS), Pittsburgh, PA, 1994. p 323-328.
  26. Machi J, Sigel B. Ultrasound for Surgeons. New York, NY: Igaku-Shoin Medical Publishers Inc., 1997.
  27. Lisle DA. Imaging for Surgeons (2<sup>nd</sup> edition). New York, NY: Oxford University Press, Inc., 1999.
  28. Webb S, editor. The Physics of Medical Imaging. Philadelphia, PA: IOP Publishing Ltd, 1988.
  29. Tempkin BB. Ultrasound Scanning. Philadelphia, PA: WB Saunders Company, 1999.
  30. Besl PJ, McKay ND. A method for registration of 3D

- shapes IEEE Trans Pattern Analysis Machine Intel 1992;14(2):239–256
- 31 Horn BKP Closed-form solution of absolute orientation using unit quaternions J Optical Soc Am A 1987;4(4):629–642
- 32 Horn BKP, Hilden HM, Negahdaripour S Closed-form solution of absolute orientation using orthonormal matrices J Optical Soc Am A 1988;5(7):1127–1638
- 33 Lucas BD, Kanade I An iterative image registration technique with an application to stereo vision Proceedings of the International Joint Conference on Artificial Intelligence, 1981 p 674–679
- 34 Blackall JM, Rueckert D, Mauer CR, Penney GP, Hill DLG, Hawkes DJ An image registration approach to automated calibration for freehand 3D ultrasound In: Delp SL, DiGioia AM, Jaramaz B, editors: Proceedings of the Third International Conference on Medical Image Computing and Computer Assisted Intervention (MICCAI 2000), Pittsburgh, PA, October 2000 Lecture Notes in Computer Science 1935 Berlin: Springer, 2000 p 462–471